Optimization of Sensor Signals for Resistive Wall Mode Control in ITER

Yueqiang Liu[1] **and J.B. Lister**[2]

[1] Department of Applied Mechanics, EURATOM/VR Fusion Association, Chalmers University of Technology, Göteborg, Sweden

[2] Association EURATOM-Confédération Suisse, Ecole Polytechnique Fédérale de Lausanne (EPFL), CRPP, CH-1015 Lausanne, Switzerland

E-mail: yueqiang.liu@chalmers.se

Abstract. Active control of the resistive wall mode has been considered as an alternative way, besides passive control by plasma rotation, to stabilize the mode in advanced scenarios in ITER. We show that a significant improvement of the feedback system is achievable by optimizing the detection system, without changing the active coil system in the design. Both analytical theory in cylindrical geometry, and toroidal calculations for ITER equilibria, show that the resistive wall mode can be stabilized for plasma pressures close to the ideal-wall beta limit, using the new technique with even radial sensors. This high plasma pressure is stabilized with the feedback coils outside the vacuum vessel, as in the nominal ITER design.

Submitted to: *Nucl. Fusion*

PACS numbers: 52.55.Tn, 52.55.Fa, 52.35.Bj, 28.52.Av, 02.30.Yy

1. Introduction

Advanced tokamak scenarios, such as the ITER Scenario-4 [1], may suffer from global ideal MHD instabilities - the low-n (n is the toroidal mode number), non-axisymmetric resistive wall modes (RWM), which limit the operational space in terms of achievable plasma pressures under steady state operation. The RWM becomes unstable as soon as the normalized plasma pressure $\beta_N \equiv \beta(\%)a(m)B_0(T)/I_p(MA)$ exceeds the Troyon no-wall limit $\beta_N^{\mathrm{no-wall}}$ [2]. Here β is the ratio of the volume-averaged plasma kinetic pressure to the magnetic pressure, B_0 is the toroidal magnetic field at the plasma center, and I_p is the total plasma current. It is highly desirable to stabilize the RWM in ITER, especially the $n = 1$ mode that gives the most severe pressure limit for the Scenario-4.

Both theory [3, 4, 5, 6] and experiments [7, 8, 9, 10] have suggested a possibility of mode stabilization by a rapid plasma toroidal rotation, where kinetic resonance processes probably play an important role in the mode damping [11, 5, 6]. However, as indicated by our previous work [5], stabilization relying on plasma rotation may not be robust for $n = 1$ RWM control in ITER. Active control of the mode, as an alternative way, is therefore necessary.

A recent work [12] on the vertical stability control (the $n = 0$ RWM control) has suggested an idea of using a combined sensor signal, measured at various poloidal locations, as one way to improve the feedback system. A key element in this idea is to use as many sensor signals as possible, in order to extract maximally the response from the full system unstable mode. In this work, we apply the similar idea to improve the $n = 1$ RWM control in ITER. There are a few advantages with this approach. First, assuming that in an ideal case, we are able to detect the pure response of the unstable RWM, we then need *only* a controller with proportional feedback gains to stabilize the mode. No derivative gains are required (for possible compensation of the phase lag in the plasma response) even at high plasma pressures. This is highly desirable since derivative gains require the time differentiation of sensor signals, that increases the noise level in the measurement. Secondly, as we will show, this approach works efficiently for radial sensors. Previous theory [13, 14, 15, 16, 17] and experiments [18, 19, 20] have shown that, using the poloidal field component just inside the resistive wall as the sensor signal, yields a superior control scheme to the radial field sensor. However, a poloidal sensor, facing directly the plasma surface, is arguably subject to more noise pollution. A radial sensor, located just beyond the conducting wall, picks up less noise, partially because the high frequency noise is filtered out by the wall. Moreover, techniquely it might be more convenient to install radial sensors outside the vacuum vessel than poloidal sensors inside. Finally, this approach proposes an instructive way for the sensor system optimization.

The basic idea is the following. We consider a standard state-space description of the linear system for the RWM control with a controller K

$$\begin{aligned} \dot{x}_p &= A_p x_p + B_p u, \\ y &= C_p x_p + D_p u, \\ u &= -Ky, \end{aligned}$$

where x_p is a vector of physical variables representing the state of the system, normally the

currents or fields from the plasma and the resistive wall. For the RWM control, the control signal u is considered to be the current in the active coils. The sensor signal y represents the magnetic field or flux through the pick-up coils. A_p, B_p, C_p, D_p are matrices of appropriate dimensions.

Typically the matrix A_p has a single unstable eigenvalue $\gamma_0 > 0$, with all the other eigenvalues being stable. It is possible to find a matrix T that orthogonalizes the state variables $x_p = Tx$, with $x = [x_0 \quad x_s]$, such that x_0 is the state corresponding to the unstable eigenvalue γ_0, and x_s is a vector of all state variables corresponding to the stable eigenvalues of A_p. Thus, we can re-write the state-space equations as

$$\begin{bmatrix} \dot{x_0} \\ \dot{x_s} \end{bmatrix} = \begin{bmatrix} \gamma_0 & 0 \\ 0 & A_s \end{bmatrix} \begin{bmatrix} x_0 \\ x_s \end{bmatrix} + \begin{bmatrix} b_0 \\ b_s \end{bmatrix} u.$$

From the new state-space description, it is clear that the best control is $u = -Kx_0$. This is an "ideal" situation, where we assume that the sensor signal is purely the unstable state variable x_0. In this case we need only a proportional gain $K = K_p$ to stabilize the system. Due to the orthogonalization, this feedback system will not destabilize the stable states x_s.

In practice, in order to reach as close as possible the "ideal" situation, we try to find the best combination of the output signals y which estimates x_0. In other words, we look for the best sensor signal that corresponds to the response purely from the unstable RWM. We achieve this by measuring the radial or poloidal component of the magnetic fields at a few poloidal locations around the torus, and find the best linear combination of these fields, such that the response from parasitic (i.e. stable) poles cancel each other or at least minimized.

In this paper, we follow this approach based on the frequency response. The best plasma response is described by a single pole transfer function

$$P(s) \equiv \frac{\Psi_s}{M_{sf} I_f} = \frac{R}{s - \gamma_0}, \qquad \gamma_0 > 0, \tag{1}$$

where s is the Laplace variable. Ψ_s is the magnetic flux or field through the sensor loop. M_{sf} is the mutual inductance between the active and the sensor coils in free space. I_f is the total current in the active coils. R is the residue that describes how the unstable RWM, with an initial growth rate γ_0, responds to the currents in the active coils.

In practice, for a given sensor location, the response function $P(s)$, describing the dynamics of an unstable plasma, is normally a transfer function containing a few poles, with a single one being unstable. Our goal is to make a linear combination of transfer functions, constructed for different poloidal locations of sensors, as close as possible to (1).

We demonstrate this idea by assuming that the plasma response is approximated by three pole rational functions. We choose sensors at three poloidal locations (labeled as U, M, L), and obtain three transfer functions, respectively,

$$P^U(s) = \frac{R_0^U}{s - \gamma_0} + \frac{R_1^U}{s - \gamma_1} + \frac{R_2^U}{s - \gamma_2}, \qquad \gamma_0 > 0, \gamma_1 < 0, \gamma_2 < 0,$$
$$P^M(s) = \frac{R_0^M}{s - \gamma_0} + \frac{R_1^M}{s - \gamma_1} + \frac{R_2^M}{s - \gamma_2},$$

$$P^L(s) = \frac{R_0^L}{s-\gamma_0} + \frac{R_1^L}{s-\gamma_1} + \frac{R_2^L}{s-\gamma_2}.$$

We then construct a linear combination of sensor signals, resulting in a linear combination of transfer functions

$$P(s) = C_U P^U(s) + P^M(s) + C_L P^L(s).$$

We choose C_U and C_L in order to cancel exactly residues associated with γ_1 and γ_2

$$C_U R_1^U + R_1^M + C_L R_1^L = 0,$$
$$C_U R_2^U + R_2^M + C_L R_2^L = 0.$$

The total (optimal) response becomes

$$P(s) = \frac{C_U R_0^U + R_0^M + C_L R_0^L}{s-\gamma_0}.$$

We note that this approach is different from the RWM feedback system proposed for the Reversed Field Pinch (RFP) experiments, in that we do not require a full coverage of the torus surface by active coils. In fact we use only one set of active coils along the poloidal angle. Normally, we do not need a full coverage by sensor coils either. The similarity with the RFP experiments is that one tries to control a single mode in both cases - in the RFP machine T2R, convincingly successful RWM control has been achieved by stabilizing each *single* (m,n)-instability individually in the Fourier space (so-called mode control) [21], whereas in tokamaks, the approach proposed here tries to stabilize a *single* unstable RWM, by decoupling it from all stable RWMs using sensor optimization. The single unstable mode in tokamaks consists of many Fourier harmonics due to the toroidal coupling.

This approach resembles the approach of using filtering techniques in [16]. However, our approach offers a more instructive way to improve the sensor signals.

For simplicity, we consider the so-called current control with ideal power supplies. We also neglect the effect of plasma rotation. The same technique applies while including non-ideal effects, voltage control and plasma rotation.

In Section 2, we show the optimization technique for a cylindrical plasma, where the transfer functions for the plasma response are constructed analytically. Section 3 reports the optimization results for an ITER plasma from the advanced scenario. The cylindrical theory, besides the important conclusions from itself, also offers a benchmark of the conclusions from the toroidal calculations. We summarize the results in Section 4.

2. Sensor optimization in cylindrical geometry

2.1. Formulations

In [15, 22], we analytically constructed transfer functions for the plasma response, for a cylindrical plasma with circular cross-section and a step-function current density profile. The plasma response can be written as

$$P(s) = \sum_m M^m(s) f_m \exp(-jm\theta_s),$$

where $f_m = m\sin(m\theta_f)(r_w^2 + r_f^2 - 2r_w r_f \cos\theta_f)/(2|m|r_f^2 \sin\theta_f)$ is a geometrical coupling factor between the active coil and the mid-plane sensor, θ_f is half of the poloidal coverage by the active coil, θ_s is the poloidal angle of the (pointwise) sensor location. The geometry of the feedback system is shown in Fig. 1. The function $M^m(s)$ contains a single pole γ_m, and is computed for each individual Fourier harmonic m, for both external and internal active coils, as well as for radial and poloidal sensors [22]. A good convergence is obtained by including Fourier harmonics from $m = -40$ to 40, of which only one mode, $m = m_0$ ($m_0 = 3$ in this study), is unstable.

For a cylindrical equilibrium, the instability ($\gamma_{m_0} > 0$) is driven by the plasma current, and determined by the choice of the safety factor at the plasma center, q_0. We choose q_0 such that the growth rate γ_{m_0} matches that for a typical toroidal plasma, with a given scaling factor for the plasma pressure $C_\beta \equiv (\beta_N - \beta_N^{\mathrm{no-wall}})/(\beta_N^{\mathrm{ideal-wall}} - \beta_N^{\mathrm{no-wall}})$. This way, we interpret instability of the RWM for the cylindrical case, in terms of the equivalent C_β. Figure 2 shows the correspondence between the mode growth rate, q_0, and C_β.

The transfer functions, for sensors located at the mid-plane, above the mid-plane ("upper sensors"), and below the mid-plane ("lower sensors"), respectively, can be written as

$$
\begin{aligned}
P^M(s) &= \sum_m \frac{R_m^M}{s-\gamma_m}, \\
P^U(s) &= \sum_m \frac{R_m^U}{s-\gamma_m}, \quad R_m^U = R_m^M \exp(-jm\theta_s), \\
P^L(s) &= \sum_m \frac{R_m^L}{s-\gamma_m}, \quad R_m^L = R_m^M \exp(jm\theta_s).
\end{aligned}
$$

A linear combination of sensor signals $\psi_s = C_U\psi_s^U + \psi_s^M + C_L\psi_s^L$ yields a transfer function $P(s) = C_U P^U(s) + P^M(s) + C_L P^L(s)$. We note that in the case of many poles in transfer functions, as in the cylindrical case (80 poles in total in each transfer function), an exact cancellation of the contribution from all stable poles is not possible anymore by combining three sensors.

In order to find an optimal combination of sensor signals, we minimize the contribution from all parasitic (stable) poles $m \neq m_0$, for a bandwidth of real frequencies $\omega(s = j\omega)$,

$$
\min_{\{C_U, C_L\}} F \equiv \left\{ \int w(\omega) \left| \sum_{m \neq m_0} \frac{C_U R_m^U + R_m^M + C_L R_m^L}{j\omega - \gamma_m} \right|^2 d\omega \right\}^{1/2}, \tag{2}
$$

where the weighting factor $w(\omega)$ is normally chosen to emphasize the low frequency contributions. The optimization results are not very sensitive to the choice of $w(\omega)$.

As the figure of merit, we define a "pollution factor" $p.f. \equiv F/F_0$, where F_0 is similar to F, but including the contribution from the unstable pole as well. The pollution factor measures the contribution from all parasitic poles to the total sensor signal. A small value of $p.f.$ indicates a better detection of the response purely from the unstable pole.

2.2. Optimization results

The cylindrical theory allows an easy investigation of the sensor optimization for various choices of model parameters, including the wall radius r_w, the radius of the active coils r_f, the poloidal coverage of the active coils $2\theta_f$, the poloidal location of the sensor coils θ_s, the RWM instability parameter C_β, as well as the sensor types. In this study, we fix the wall distance at $r_w = 1.3a$, where a is the plasma minor radius. We consider active coils located either outside ($r_f = 1.5a$, external coils) or inside ($r_f = 1.25a$, internal coils) the resistive wall. We fix $\theta_f = 0.2\pi$, and vary both θ_s and C_β. We carry out the optimization for both radial and internal poloidal sensors (poloidal sensors located on the inner side of the resistive wall). We do not consider poloidal sensors located outside the wall (external poloidal sensors), because these are much worse than the internal ones [15], due to the poloidal field jump caused by eddy currents in the wall. Since the radial component of the magnetic field is continous across a (thin) wall, radial sensors can be located just inside or just outside the wall.

As the first example, Fig. 3 shows the results, in terms of the Nyquist plots for transfer functions, with external coils and radial sensors, for $C_\beta = 0.5$ and $\theta_s = 0.15\pi$. A Nyquist plot of the transfer function $P(s)$ is the complex plot of $P(j\omega)$ for real frequencies ω. If the open-loop transfer function $P(s)$ has only one unstable pole, the Cauchy principle of phase variation states that, the closed loop, with a stable controller $K(s)$, is stable if and only if the corresponding Nyquist curve $K(j\omega)P(j\omega)$ encircles -1 once in the counter clock-wise direction, as the frequency ω varies from $-\infty$ to $+\infty$. For the transfer functions shown in Fig. 3(a-c), for upper, lower, and mid-plane sensors, respectively, it can be verified that any standard stable controllers with proportional, derivative, and integral actions (PID-controllers) can not stabilize the mode. However, the linear combination of three sensor signals (i.e. the linear combination of three transfer functions shown in (a-c)), as a result of solving the optimization problem (2), yields a transfer function that can easily be stabilized by a proportional controller, with the gain slightly larger than 1 for a marginal stability (a good control with a sufficient stability margin requires a gain of about 2), as shown by Fig. 3(d). [In this study, the feedback gain is defined as $-\Psi_s^{\rm vac}/\Psi_s$, where $\Psi_s^{\rm vac} \equiv M_{sf} I_f$ is the *radial* sensor signal due to the vacuum field produced by active coils, Ψ_s is the (total) sensor signal in the presence of the plasma and wall. The characteristic equation for the closed loop is $1 + K(s)P(s) = 0$.] Thus we obtain a qualitative improvement for the mode control, by combining the radial sensors in an optimal manner. In contrary, we find only quantitative improvement for internal poloidal sensors, because the mid-plane poloidal sensors alone also allow stabilization of the mode using a proportional controller.

The results in Fig. 3 are better understood by comparing the amplitude of sensor signals for the mid-plane sensor and the optimally combined sensor, as shown in Fig. 4. In the rest of this study, we always choose the mid-plane sensor as a reference while evaluating the performance of the optimal one. The reason is that the outboard mid-plane sensor gives a better detection of the plasma response than sensors at other poloidal locations, thanks to the ballooning nature of the high-pressure driven RWM in a torus. For mid-plane sensors, Fig. 4 shows that the amplitude of parasitic contributions is even larger than that of the total at low

frequencies. This results in a positive value for $\mathrm{Re}[P(j\omega)]$ at $\omega = 0$, as shown in Fig. 3(b), which makes the stabilization impossible with a PID controller. For the optimal combination of sensors, the parasitic contribution is significantly reduced, without reducing the total signal. This yields a transfer function close to the single pole approximation, and the corresponding Nyquist curve is close to a circle as shown in Fig. 3(d).

Similar results are obtained for other choices of parameters. Figure 5 shows the pollution factor as a function of C_β, for mid-plane radial sensors compared with optimal radial sensors, with $\theta_s = 0.15\pi, 0.2\pi, 0.3\pi$. The optimization is performed for each C_β and θ_s separately. A qualitative improvement is achieved, as the pollution factor is reduced from the order of 1 to the order of 0.1. We also notice that the optimization becomes harder when increasing the plasma pressure, as expected.

An easy way to illustrate the qualitative improvement of control for radial sensors, is to compare the maximal achievable C_β for various choices of sensor configurations. Figure 6 shows the minimum proportional gain required for stabilization of the mode, using mid-plane sensors and optimal sensors, for the same coil configurations as in Fig. 5. The maximal achievable C_β are about 1.0, 0.9, 0.78, for $\theta_s = 0.15\pi, 0.2\pi, 0.3\pi$, respectively. This is significantly better than the mid-plane radial sensors, which stabilize the mode only for C_β up to 0.1.

Figure 7 shows the optimal coefficient C_U in the complex plane, for upper coils. The coefficient for lower coils satisfies $C_L = \mathrm{conj}(C_U)$, and the coefficient for mid-plane coils is specified *a-priori* $C_M = 1$. The optimal solution depends strongly on the choice of θ_s. However, for a given θ_s, the dependence on C_β is rather weak, which is a good property for the purpose of robust control against the plasma pressure.

The sensitive dependence of the optimal solution on θ_s should not be a significant issue in practice, since the coil configuration is already fixed in the design phase. In order to find the best sensor configuration in terms of θ_s, we optimize the linear combination for a range of θ_s. Figure 8 compares the pollution factors versus θ_s, for the optimal sensors and the mid-plane sensors. The optimization is made for each individual θ_s. We observe a wide window in $\theta_s \simeq 0.1\pi - 0.33\pi$, in which the RWM can be stabilized using the sensor optimization. It is interesting to notice that at the left and right boundaries of the solid curve in Fig. 8, the sensor signals become almost linearly dependent. Therfore, due to the almost complete cancellation, including even the response from the unstable pole, the total response becomes almost zero for all frequencies.

We also made the sensor optimization for internal poloidal sensors. The results are similar to that of radial sensors, except the following. (1) The sensor optimization yields rather quantitative, than qualitative, improvement of the control for poloidal sensors. By quantitative improvement, we mean that the system parameters have changed, but the fundamental ability to stabilize has not changed. By qualitative improvement, we mean that the system parameters have changed in such a way as to go from non-stabilizable to stabilizable. An internal poloidal sensor, located at the outboard mid-plane, already gives stabilization of the RWM for high plasma pressures, thanks to the fact that the parasitic contribution of the stable poles is already small compared to the total sensor signal. As an example, Fig. 9 shows the pollution factors

versus C_β for the mid-plane poloidal sensors and the optimized poloidal sensors, for various choices of θ_s. For the cylindrical equilibria considered here, the pollution factors are already below 0.1 with mid-plane sensors. (2) The values of optimal coefficient C_U are less clustered with increasing C_β. (3) An even wider stabilization window in θ_s, than for radial sensors, is observed for poloidal sensors.

Finally, we note that the same technique also works for internal active coils ($r_f = 1.25a < r_w$), as should be expected. We illustrate this by showing the optimization results for radial sensors. Figure 10 shows the pollution factors with increasing C_β for $\theta_s = 0.15\pi, 0.2\pi, 0.3\pi$. A reduction of $p.f.$ from order 1 to order 0.1 is again achieved, resulting in a qualitative improvement of the mode control using radial sensors.

3. Sensor optimization in ITER

3.1. Equilibrium and feedback configuration

Figure 11 shows the geometry of the RWM control using the proposed scheme, for an ITER steady state scenario (Scenario-4). This scenario has weak negative magnetic shear and a highly shaped plasma, with the designed total plasma current 9MA, and 340MW fusion power production at $Q = 5$ [1]. The target plasma is marginally unstable, with C_β about 0.1. We model the ITER double wall and the plasma facing component (the blanket modules) as axisymmetric thin shells. The active coils are super-conducting side correction saddle coils from the present ITER design. Three sets of *radial sensors* are located on the inner wall, at three poloidal angles as shown in the figure. The locations of the upper and lower sensors are chosen by taking into account the cylindrical results.

We scale the plasma pressure from the ITER target equilibrium, in order to obtain a full range of beta from the no-wall to the ideal-wall limits, while keeping the total plasma current at 9MA. Using the MHD stability code MARS-F [13], we computed the no-wall β_N limit, for marginal stability of the $n = 1$ external ideal kink, as 2.45, and the ideal-wall limit as 3.65 (assuming the ITER inner wall as ideal) [5].

3.2. Robust design

Contrary to the cylindrical case, where we optimize the linear combination of sensor signals for each individual C_β, for the ITER toroidal equilibria, we try to find a linear combination of sensor signals, that gives the best control for all plasma pressures up to the ideal-wall limit. We call this a robust design (robust against the plasma pressure). [We recall that the individual optimization in a cylinder shows that the optimal coefficients in the linear combinations are not sensitive to the variation of C_β, as shown by Fig. 7.] We choose 7 equilibria, with a successive increase of the plasma pressure: $C_\beta = 0.10, 0.22, 0.35, 0.47, 0.60, 0.73, 0.86$. We consider only radial sensors for two reasons:- (i) our previous study [5] has shown that a single set of internal poloidal sensors, located at the outboard mid-plane of the torus, is capable of stabilizing the mode for plasma pressures close to the ideal-wall limit; (ii) the cylindrical results from Section 2 indicate that only a quantitative improvement is achieved for poloidal

sensors using this optimization technique, whereas the improvement is qualitative for radial sensors.

Let us denote the transfer function for the sensor q at pressure $C_\beta^{(k)}$ as

$$P_k^q(s) = \sum_{m=0}^{M} \frac{R_{km}^q}{s-\gamma_{km}}, \qquad q = 1,\cdots Q; \quad k = 1,\cdots 7.$$

We assume the sensor $q = Q$ is the "main" sensor (the mid-plane one in this study, with Q=3). We also assume that the pole $m = 0$ is the unstable one ($\gamma_{k0} > 0, \gamma_{k,m>0} < 0$). As before [5], we find that three-pole (i.e. $M = 2$) rational functions yield good approximations for all transfer functions $\{P_k^q(s)\}$. We computed all the poles $\{\gamma_{km}\}$ and residues $\{R_{km}^q\}$ as the basis for the sensor optimization.

We then look for a set of coefficients $\{C_q\}$, that are independent of the plasma pressure, and give "optimal" transfer functions for all plasma pressures $C_\beta^{(k)}$

$$P_k(s) = \sum_{q=1}^{Q} C_q P_k^q(s), \qquad (C_Q = 1).$$

Similar to the cylindrical case, for each $C_\beta^{(k)}$, we generalize (2) and define a function

$$F_i^{(k)} \equiv \left\{ \int w^s(\omega) \left| \sum_{q=1}^{Q} \sum_{m=i}^{M} C_q \frac{R_{km}^q}{j\omega - \gamma_{km}} \right|^2 d\omega \right\}^{1/2}, \qquad (C_Q = 1).$$

The "pollution factor" ($p.f.$) for each pressure $C_\beta^{(k)}$ is

$$p.f.(k) \equiv \frac{F_1^{(k)}}{F_0^{(k)}}, \tag{3}$$

which is a quantitative measure of the contribution of the response from all stable poles, to the total plasma response.

For a robust design, we specify the goal function for the optimization as a weighted sum of $p.f.$ for all chosen plasma pressures

$$\min_{\{C_q\}} \sum_k w_k^c \;\; p.f.(k), \tag{4}$$

where the weighting factors are chosen as

$$w_k^c = 1, \qquad w^s(\omega) = \sum_k w_k^c \left| \sum_{m=1}^{M} \frac{R_{km}^Q}{j\omega - \gamma_{km}} \right|^2.$$

Note that had we optimized $\{C_q\}$ for each individual plasma pressure $C_\beta^{(k)}$, we always obtained an exact cancellation of the parasitic contributions, as illustrated in introduction. Therefore, the pollution factor, as defined in (3), always vanished.

3.3. Optimization results

We carried out the sensor optimization for the ITER plasma according to (4), based on three-pole transfer functions computed for all radial sensors and all plasma pressures. Figure 12 shows the pollution factors versus the plasma pressure, for both the mid-plane sensors and the optimal sensors. A reduction of the pollution factors, generally by a factor of 5, is achieved. With the optimal combination, the pollution factor is less than 0.36 for all pressures. This quantitative reduction results in a qualitative improvement of the control, as will be shown by Fig. 15. We emphasize here that a single, optimal combination works for all plasma pressures up to $C_\beta = 0.86$, indicating a robust design is possible. A close examination of the results reveals that the choice of optimal C_U and C_L is mainly determined by the plasma response at the highest pressure $C_\beta = 0.86$. Inversely, we find that an optimal combination that works for a high plasma pressure, also generally works for lower pressures. This is identical to the modelled and observed behaviour of n=0 stabilization.

We investigated how sensitive the departure from the optimum affects the results. Figure 13 shows a contour plot of the maximal pollution factor in the complex plane for $C_U \equiv C_1$ (the coefficient for the upper sensor). The coefficient for the lower sensor $C_L \equiv C_2$ is determined by an *ad hoc* chosen linear relation to C_U. A slight variation of the coefficient C_U around the optimum does not yield a significant increase of the pollution factor, for all pressures.

Figure 14 shows the Nyquist plots of the transfer functions for various plasma pressures, for mid-plane radial sensors, and the optimal linear combinations of three radial sensors as the result of the robust design. At lower pressures (Fig. 14(a-b)), the stability criterion determines that, using radial mid-plane sensors (curves "1") stabilizes the $n = 1$ RWM with large enough proportional feedback gains. The optimization of radial sensors (curves "2") improves the mode control quantitatively by reducing the critical gains. At higher pressures (Fig. 14(c-d)), radial mid-plane sensors do not allow stabilization of the mode with any stable PID controllers. However, optimized combinations of radial sensors allow stabilization with large enough proportional gains, resulting in a qualitative improvement of the mode control. We also notice that the optimized sensor signals (the amplitude of the transfer functions) become smaller with increasing C_β. As a consequence, we need more proportional gain to stabilize the mode, as the plasma pressure increases.

Summarizing the optimization results for all chosen pressures for ITER, we plot the critical proportional gain versus C_β in Fig. 15. With mid-plane sensors only (dashed line), the mode stabilization is possible for C_β up to about 0.4, whereas the optimal combination of radial sensors expands the stabilization boundary up to $C_\beta \simeq 0.9$.

We mention that similar results have also been obtained by studying other toroidal plasmas than ITER. In this study, we try to find a robust solution for the sensor optimization. However, even better results (in terms of the maximum achievable C_β and the control performance) can be achieved by performing the optimization for each plasma pressure individually. We also considered sensor optimization using five sets of radial sensors along the poloidal angle. The additional benefit, compared with that from three sets of sensors, is not significant.

4. Conclusions

Both toroidal calculations and cylindrical theory show, that significant improvement of the RWM control can be achieved, by choosing an optimal linear combination of sensor signals at different poloidal locations. This technique works for both radial and poloidal sensors, with both external and internal active coils. The improvement for radial sensors is qualitative. With optimal choice of linear combinations, stabilization of RWM up to ideal wall beta limit, using only proportional gains, is possible with radial sensors. For the advanced scenario in ITER, a robust design for feedback stabilization of the $n = 1$ RWM is possible, using an optimal linear combination of radial sensors. A single set of optimally chosen coefficients in the linear combination works for all plasma pressures up to $C_\beta = 0.86$. These results are obtained for active coils outside the ITER vacuum vessel.

Acknowledgments

Very helpful discussions with Dr. M.S. Chu from General Atomics, and Dr. M. Okabayashi from Princeton Plasma Physics Laboratory, are gratefully acknowledged. This work, supported by the European Communities under the contract of the Association between EURATOM/VR, was carried out within the framework of the European Fusion Development Agreement. The views and opinions expressed herein do not necessarily reflect those of the European Commission.

References

[1] Polevoi A. et al., Fusion Energy 2002 (Proc. 19th Int. Conf. Lyon, 2002) (Vienna: IAEA) CD-ROM file CT/P-08 and http://www.iaea.org/programmes/ripc/physics/fec2002/html/fec2002.htm
[2] Troyon F., et al., Plasma Phys. Controll. Fusion **26**, 209 (1984).
[3] Bondeson A. and Ward, D.J., Phys. Rev. Lett. **72**, 2709 (1994).
[4] Chu M.S., et al., Phys. Plasmas **2**, 2236 (1995).
[5] Liu Y.Q., et al., Nucl. Fusion **44**, 232 (2004).
[6] Hu B. and Betti R., Phys. Rev. Lett. **93**, 105002 (2004).
[7] Garofalo A.M., et al., Phys. Rev. Lett. **82**, 3811 (1999).
[8] La Haye R.J., et al., Nucl. Fusion **44**, 1197 (2004).
[9] Sabbagh S.A., et al., Nucl. Fusion **46**, 635 (2006).
[10] Reimerdes H., et al., Phys. Plasmas **13**, 056107 (2006).
[11] Bondeson A. and Chu M.S., Phys. Plasmas **3**, 3013 (1996).
[12] Favez J-Y., et al., Plasma Phys. Control. Fusion **47**, 1709 (2005).
[13] Liu Y.Q., et al., Phys. Plasmas **7**, 3681 (2000).
[14] Pustovitov V.D., Plasma Phys. Control. Fusion **44**, 295 (2002).
[15] Bondeson A., et al., Phys. Plasmas **9**, 2044 (2002).
[16] Chu M.S., et al., Nucl. Fusion **43**, 441 (2003).
[17] Liu Y.Q., et al., Phys. Plasmas **13**, 056120 (2006).
[18] Garofalo A.M., et al., Nucl. Fusion **41**, 1171 (2001).
[19] Okabayashi M., et al., Phys. Plasmas **8**, 2071 (2001).
[20] Strait E.J., et al., Nucl. Fusion **43**, 430 (2003).
[21] Brunsell P.R., et al., Phys. Rev. Lett. **93**, 225001 (2004).

[22] Liu Y.Q., Plasma Phys. Control. Fusion **48**, 969 (2006).

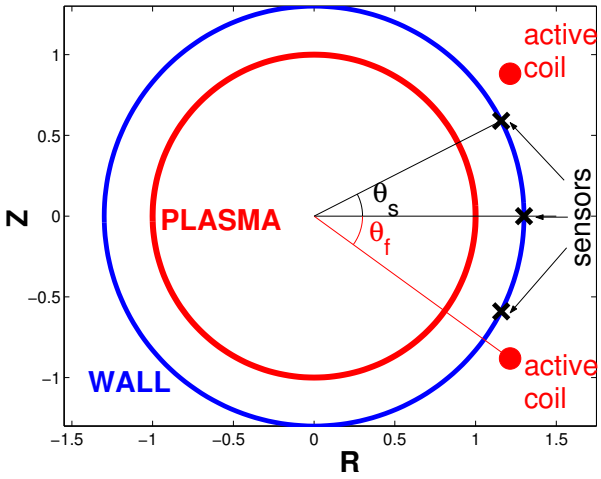

Figure 1. Geometry of the RWM control in a cylinder, using multiple sensors. The feedback system consists of one set of active coils along the poloidal angle, with a poloidal coverage $2\theta_f$, and three sets of (pointwise) sensors on the wall, located at poloidal angles $\theta_s, 0$, and $-\theta_s$, respectively.

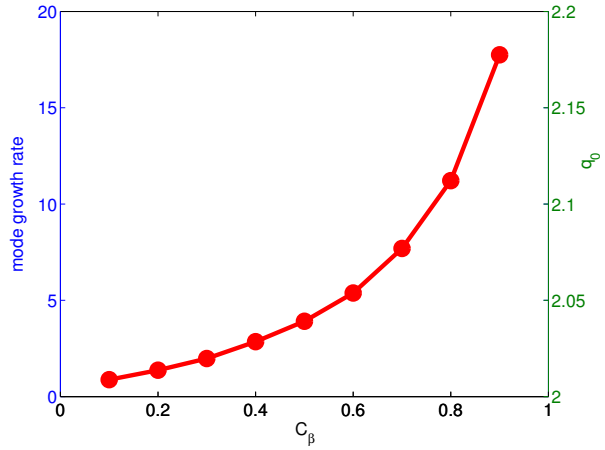

Figure 2. A sequence of cylindrical equilibria, with increasingly more unstable RWM, is characterized by a parameter C_β, defined for a typical toroidal equilibrium. The growth rates of the RWM are matched between the cylindrical and toroidal equilibria.

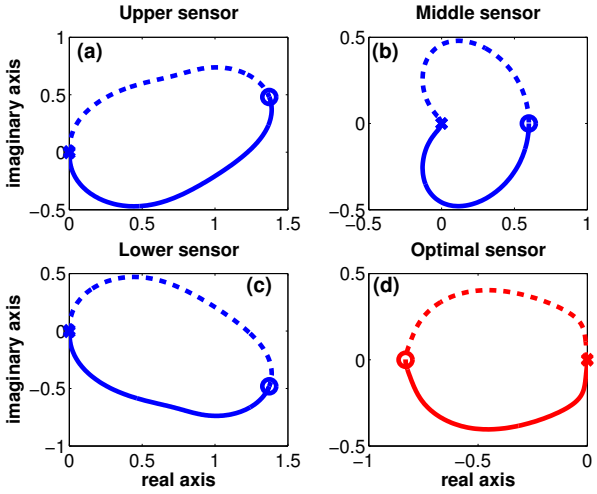

Figure 3. Transfer functions $P(j\omega)$ from cylindrical theory, plotted in the complex plane for real frequencies $-\infty < \omega < +\infty$, for (a) - upper radial sensors, (b) - mid-plane radial sensors, (c) - lower radial sensors, and (d) - the optimal linear combination of radial sensors. Solid lines correspond to $\omega > 0$, and dashed lines correspond to $\omega < 0$. Other parameters are chosen as $r_f = 1.5a, r_w = 1.3a, \theta_f = 0.2\pi, \theta_s = 0.15\pi, C_\beta = 0.5$.

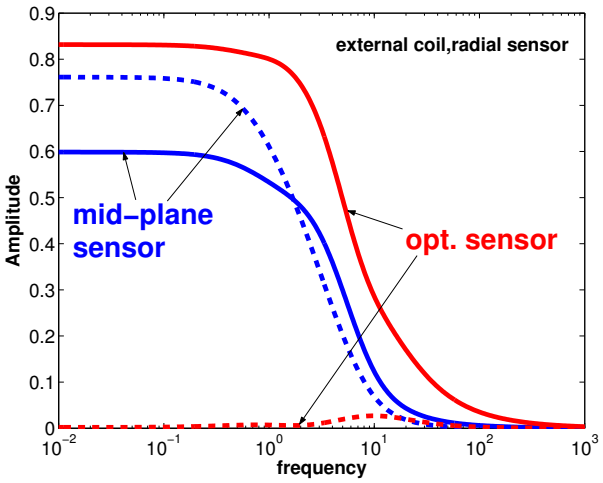

Figure 4. Comparisons of the amplitude, as functions of frequency ω, of the total sensor signal (solid lines) with that contributed by parasitic (stable) modes (dashed lines). Shown for a cylindrical case with $r_f = 1.5a, r_w = 1.3a, \theta_f = 0.2\pi, \theta_s = 0.15\pi, C_\beta = 0.5$.

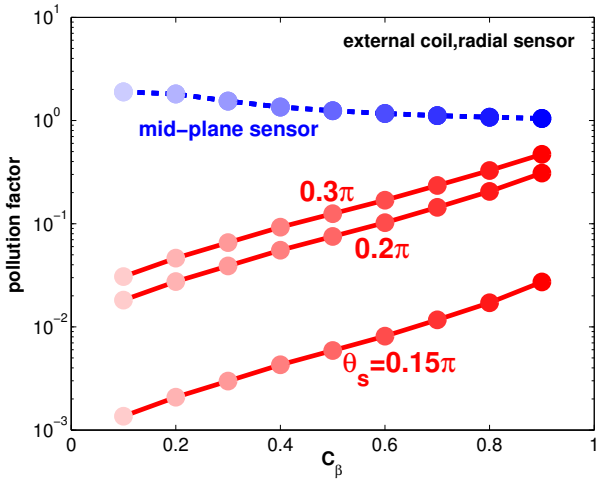

Figure 5. Comparisons of the pollution factors for mid-plane radial sensors (dashed line) and optimal radial sensors (solid lines), with increasing plasma pressure C_β and various choices of off-mid-plane sensor locations θ_s. Shown for a cylindrical case with $r_f = 1.5a, r_w = 1.3a, \theta_f = 0.2\pi$.

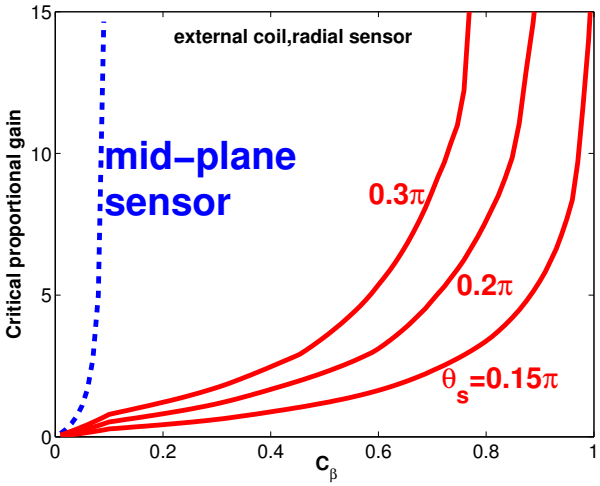

Figure 6. Critical proportional gains for a marginal stabilization of the RWM versus C_β, for mid-plane radial sensors (dashed line) and optimal radial sensors (solid lines) with various choices of off-mid-plane sensor locations θ_s. Shown for a cylindrical case with $r_f = 1.5a, r_w = 1.3a, \theta_f = 0.2\pi$.

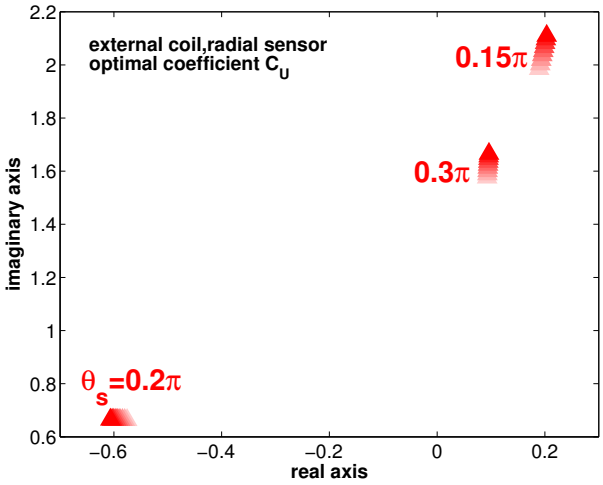

Figure 7. Complex plot of the optimal coefficient C_U for the upper sensors, in the linear combination of sensor signals. Shown for a cylindrical case with $r_f = 1.5a, r_w = 1.3a, \theta_f = 0.2\pi$, and various choices of $\theta_s = 0.15\pi, 0.2\pi, 0.3\pi$. For a given θ_s, the optimal values of C_U are well clustered as C_β varies.

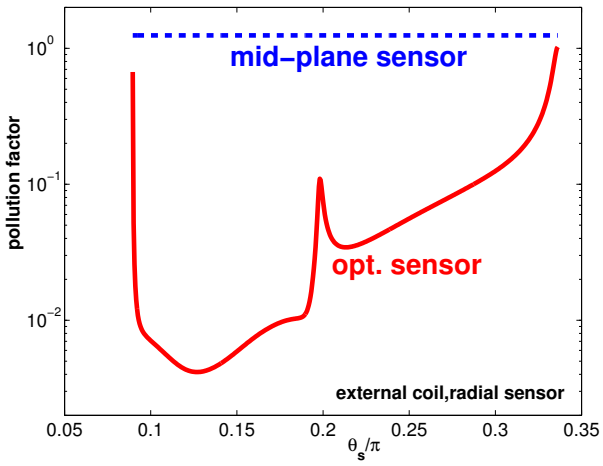

Figure 8. Comparisons of the pollution factors for mid-plane radial sensors (dashed line) and the optimal linear combination of radial sensors (solid line), for varying θ_s. Shown for a cylindrical case with $r_f = 1.5a, r_w = 1.3a, \theta_f = 0.2\pi, C_\beta = 0.5$.

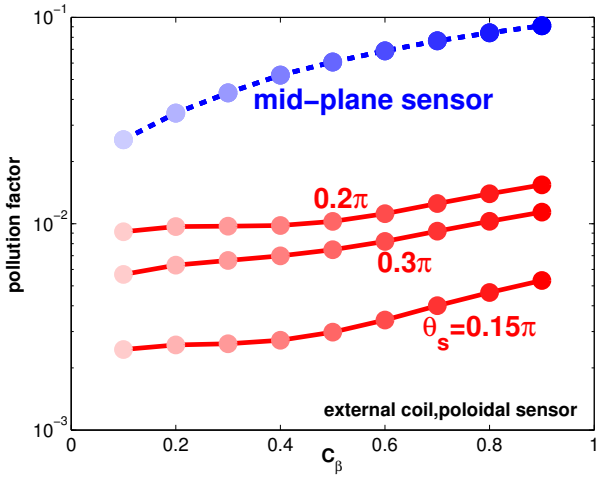

Figure 9. Comparisons of the pollution factors for mid-plane internal poloidal sensors (dashed line) and optimal poloidal sensors (solid lines), with increasing plasma pressure C_β and various choices of off-mid-plane sensor locations θ_s. Shown for a cylindrical case with $r_f = 1.5a, r_w = 1.3a, \theta_f = 0.2\pi$.

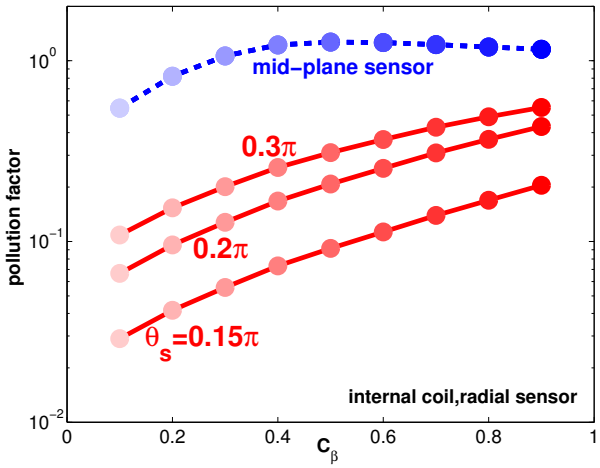

Figure 10. Comparisons of the pollution factors for mid-plane radial sensors (dashed line) and optimal radial sensors (solid lines), with increasing plasma pressure C_β and various choices of off-mid-plane sensor locations θ_s. Shown for a cylindrical case with $r_f = 1.25a, r_w = 1.3a, \theta_f = 0.2\pi$.

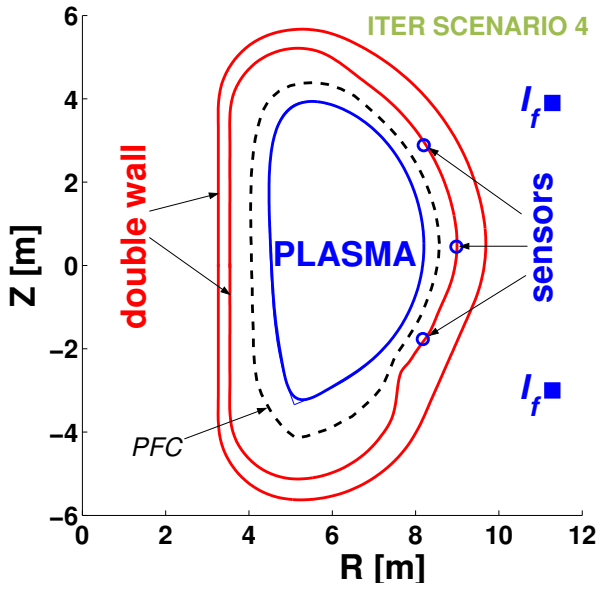

Figure 11. Geometry of the feedback system for the RWM control in ITER. The ITER double wall and the plasma facing component (the blanket) are modeled by thin shells, with the equivalent field penetration time corresponding to the ITER design. The active coils model the side correction saddle coils. The poloidal location for three sets of sensor coils ('o') are fixed in this study.

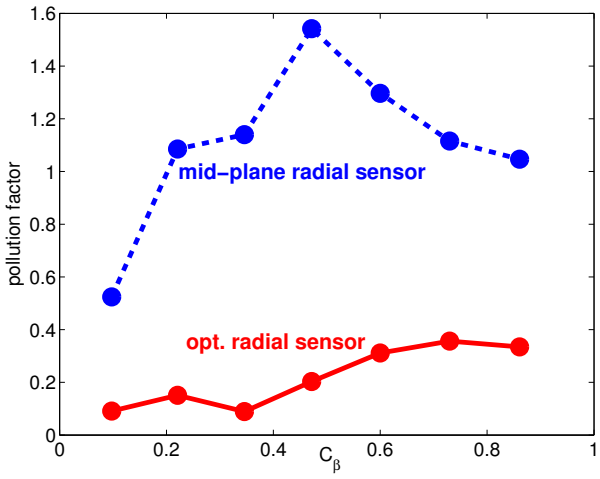

Figure 12. Comparison of the pollution factors for the mid-plane radial sensors (dashed line) and the optimal combination of radial sensors (solid line) in ITER. The optimization is made for all plasma pressures $C_\beta = 0.10, 0.22, 0.35, 0.47, 0.60, 0.73, 0.86$, resulting in optimal values for the coefficients $C_U = -1.2$ (upper sensors) and $C_L = -1.51 - 0.65\,j$ (lower sensors). The coefficient for the mid-plane sensor is fixed at $C_M = 1$.

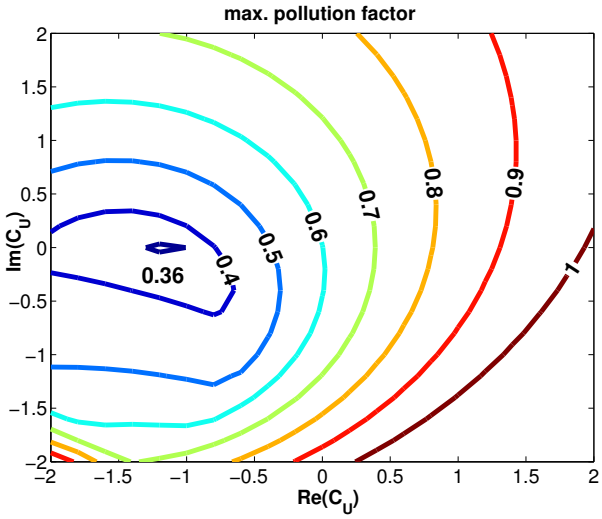

Figure 13. Contour plot of the maximal pollution factor (over all chosen pressures for the ITER plasma) in the complex plane for C_U. The coefficient C_L is determined by an *ad hoc* chosen linear relation $aC_U + bC_L = c$, with $a = 0.973 - 0.881\,j, b = 0.334 + 0.678\,j, c = -1.231 - 0.184\,j$.

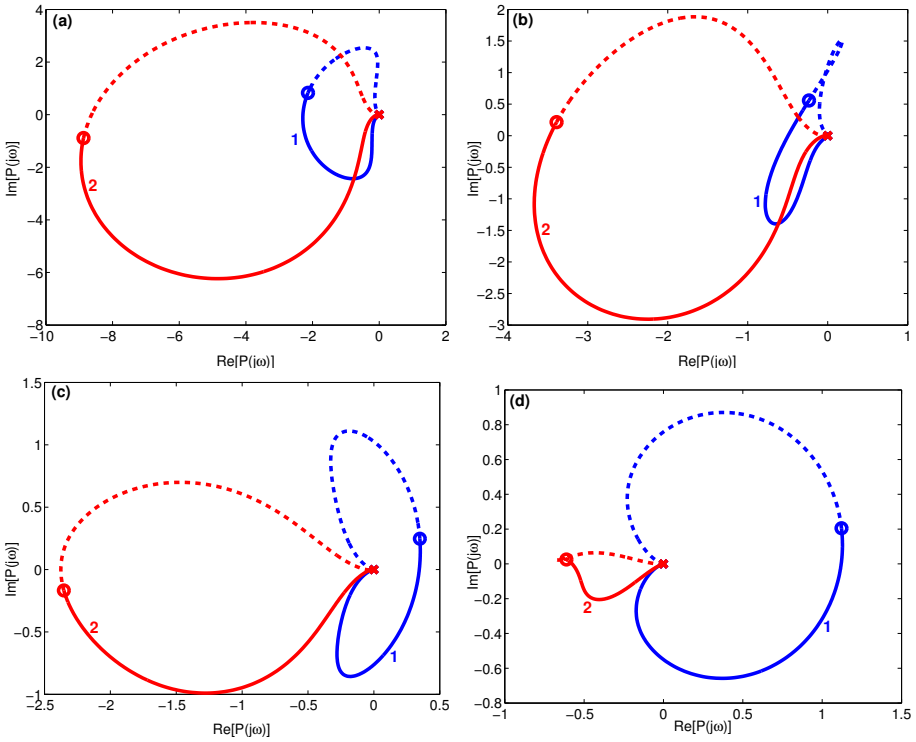

Figure 14. Comparisons of transfer functions for mid-plane radial (labeled "1") and optimal radial sensors (labeled "2") in ITER, plotted in the complex plane for real frequencies $-\infty < \omega < +\infty$, for various plasma pressures (a) - $C_\beta = 0.10$, (b) - $C_\beta = 0.22$, (c) - $C_\beta = 0.47$, (d) - $C_\beta = 0.73$. Solid lines correspond to $\omega > 0$, and dashed lines correspond to $\omega < 0$.

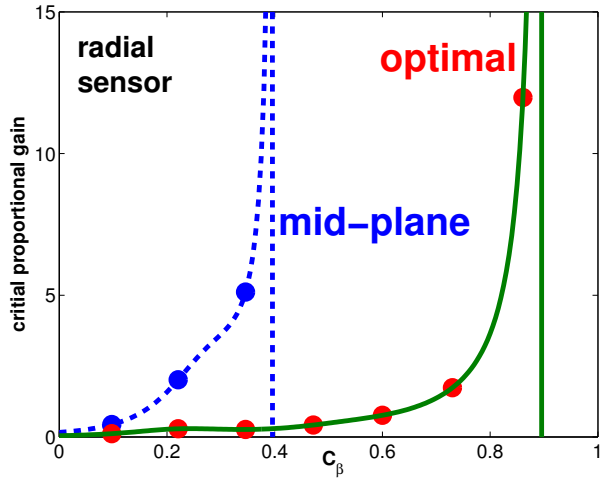

Figure 15. Comparisons of critical proportional gains, required for a marginal stabilization of the $n = 1$ RWM in ITER, versus C_β, for mid-plane radial sensors (dashed line) and the optimal linear combination of radial sensors (solid lines) at three poloidal locations.